Biochemistry (Moscow), Vol. 70, No. 7, 2005, pp. 790-798. Translated from Biokhimiya, Vol. 70, No. 7, 2005, pp. 957-967.

Originally published in Biochemistry (Moscow) On-Line Papers in Press, as Manuscript BM04-164, December 5, 2004.

Conformational Stability and Hemolytic Activity of Actinoporin RTX-SII from the Sea Anemone *Radianthus macrodactylus*

T. I. Vakorina*, E. V. Klyshko, M. M. Monastyrnaya, and E. P. Kozlovskaya

Pacific Institute of Bioorganic Chemistry, Far East Branch of the Russian Academy of Sciences, pr. 100-let Vladivostoku 159, 690022 Vladivostok, Russia; fax: (4232) 31-4050; E-mail: vakorina@piboc.dvo.ru

Received July 2, 2004
Revision received September 14, 2004

Abstract—The spatial organization of actinoporin RTX-SII from the sea anemone *Radianthus macrodactylus* on the level of tertiary and secondary structures was studied by UV and CD spectroscopy and intrinsic protein fluorescence. The specific and molar extinction coefficients of RTX-SII were determined. The percentages of canonical secondary structures of actinoporin were calculated. The tertiary structure of the polypeptide is well developed and its secondary structure is highly ordered and contains about 50% antiparallel folded β-sheets. The irreversible thermal denaturation of RTX-SII was studied by CD spectroscopy; a conformational transition occurs at 53°C. Above this temperature irreversible conformational changes are observed in the secondary and tertiary structures. This is accompanied by redistribution of the content of regular and distorted forms of β-sheet and also by increase in the content of an unordered form. It is suggested that an intermediate is formed in the process of thermal denaturation. Acid–base titration of RTX-SII results in irreversible conformational changes at pH below 2.0 and above 12.0. As shown by intrinsic protein fluorescence, tyrosine residues of RTX-SII make a fundamental contribution to emission, and the total fluorescence depends more on temperature and ionic strength of the solution than tryptophan fluorescence. The data on conformational stability of actinoporin are correlated with data on its hemolytic activity. Activity of RTX-SII significantly decreases at increased temperature and slightly decreases at low pH. Hemolytic activity drastically increases at high pH. Increase in the actinoporin activity at pH above 10 seems to be caused by ionization of the molecule.

Key words: actinoporin, secondary and tertiary structures, UV spectroscopy, circular dichroism, intrinsic protein fluorescence, hemolytic activity

Sea anemones (Coelenterata) produce various toxins of polypeptide nature [1]. Although their roles have not been clearly elucidated, it is supposed that they provide protection against predators and also serve for digestion [2]. Powerful membranolytic pore-forming cytotoxins (or actinoporins) are the main components of the sea anemone venom. Their physiological action is due to their ability to form cation-selective ion channels (pores) in sphingomyelin-containing lipid membranes of eucaryotes. This seems to be the origin of their hemolytic, cytotoxic, cardiotropic, anti-parasitic, and other types of biological activity [3, 4]. Actinoporins are of particular interest as promising anti-tumor and anti-parasitic agents [5, 6]. They serve as useful model objects when studying lipid–protein and protein–protein interactions in membranes [7-9].

More than 30 actinoporins have been isolated as isoforms from more than 22 Actiniidae and Stichodactylidae families [1-3, 10]. They are basic (isoelectric point more than 9) sphingomyelin-inhibited polypeptides with molecular mass 18-20 kD. The absence of cysteine residues is typical of their amino acid content. The degree of homology of amino acid sequence of actinoporins isolated from various sea anemone species varies from 60 to 100% [10]. The biochemical properties, structures, and functions of equinatoxins EqtI, EqtII, and EqtIII from *Actinia equina* [11], tenebrosines TN-A, TN-B, and TN-C from *Actinia tenebrosa* [12], sticholysins StI and StII from *Stichodactyla helianthus* [13], magnificalysins HMgI and HMgII from *Heteractis magnifica* [14], and *Radianthus* actinoporins RTX-A, RTX-S, and RTX-G from *Radianthus macrodactylus* [15] are best studied.

We isolated the new actinoporin RTX-SII from the tropical sea anemone *R. macrodactylus*; it is a basic

* To whom correspondence should be addressed.

0006-2979/05/7007-0790

polypeptide (isoelectric point ~10). Similar to other actinoporins [3, 10], the absence of cysteine residues and a high content of basic amino acid residues is typical of RTX-SII. According to the data of amino acid content, its molecular mass is 19.276 kD [16], whereas MALDI-TOF (time-of-flight mass-spectrometry with matrix-enhanced laser desorption/ionization) gives 19.28 kD. Similar to other *Radianthus* actinoporins, RTX-SII forms oligomeric pores consisting of four polypeptide molecules in the lipid bilayer. Its hemolytic activity is $3.6 \cdot 10^4$ HU/mg [16]. It is impossible to study the mechanism of action of actinoporin and its structure–function relationships if the spatial organization of the molecule and factors influencing the conformational stability of the polypeptide are unknown.

In the present work, we studied the spatial organization of RTX-SII on the tertiary and secondary levels, the effect of temperature, pH, and ionic strength on the conformational stability of polypeptide, and how the hemolytic activity of RTX-SII depends on its structure.

MATERIALS AND METHODS

Isolation and purification of actinoporin. RTX-SII was isolated from tropical sea anemone *R. macrodactylus* harvested near Seychelles. Anemones were homogenized with a threefold volume of distilled water. After 12-h extraction, the homogenate was filtered and centrifuged at 10,000*g* using a K-24 centrifuge (Janetzki, Germany). The aqueous extract was lyophilized and stored at –20°C until use. To isolate actinoporin, we used a scheme including precipitation of hemolytically active polypeptides with 80% acetone from aqueous anemone homogenate, gel filtration on a column with Akrilex P-4 from Reanal (Hungary), ion-exchange chromatography on a column with CM-32 cellulose from Whatman (England), and ion exchange HPLC (Beckman, USA) on a Ultropac TSK CM-3SW column from LKB (Sweden) [17]. Homogeneity of thus obtained actinoporin was proved by reversed-phase HPLC with Nucleosil C_{18} as the sorbent, capillary electrophoresis (Applied Biosystems, Sweden), and MALDI-TOF mass-spectrometry (Bruker, Germany). The protein concentration was determined according to Lowry [18].

Hemolytic activity of actinoporin was determined using a suspension of mouse erythrocytes in 0.005 M Tris-HCl buffer, pH 7.4, containing 0.155 M NaCl, 0.001 M KCl, and 0.01 M glucose. The hemoglobin level in the supernatant was monitored spectrophotometrically at 540 nm after centrifugation and precipitation of the erythrocytes. The amount of protein causing 50% hemolysis in 1 ml of 0.7% erythrocyte suspension (corresponding absorption is 1.51 at 720 nm) during 30 min at 37°C was taken as the hemolytic unit (HU). Lysis of 0.7% erythrocyte suspension on addition of 10 μl of 1% solution of holothurin A from sea hedgehogs *Holothuria leucospilota* (corresponding absorption is 0.8 at 540 nm) was taken as 100% hemolysis [19].

The effect of ionic strength and pH on RTX-SII activity was studied by incubation of actinoporin (27.6 ng) for 30 min at 37°C in solution with NaCl concentration from 0 to 0.8 M (the first case) and in 0.01 M sodium phosphate buffer solutions with pH from 3.88 to 10.25 (the second case). The final volume of the mixture was 20 μl. Then 1 ml of 0.7% erythrocyte suspension was added to the sample (three parallel experiments). The degree of hemolysis (%) was determined as described above compared with the control actinoporin-free samples.

The effect of temperature on RTX-SII activity was studied by incubation of actinoporin (27.6 ng) in 20 μl of 0.01 M sodium phosphate buffer, pH 7.2, at 25, 40, 50, and 60°C. Then 1 ml of 0.7% erythrocyte suspension heated to 37°C was added to the samples (three parallel experiments). The degree of hemolysis (%) was determined comparing with the actinoporin-free control samples as described above.

UV spectra were recorded using a Cecil CE 7200 spectrophotometer (Aquarus, England) in 1-cm pathlength quartz cuvettes with 1-nm spectral slit width. Correction for light scattering of actinoporin RTX-SII was applied as described by Winder and Gent [20]. The specific absorption coefficient ($A^{1\%}_{1\ cm}$) was determined using a sample of actinoporin brought to constant mass. The number of tyrosine and tryptophan residues in the RTX-SII molecule was evaluated by using the second derivative of the UV absorption spectra as described in [21].

CD spectra were recorded using a Jasco-500A spectropolarimeter (Jasco, Japan) in quartz cuvettes 1 mm (peptide spectral region) and 1 cm (aromatic spectral region) in pathlength. Before recording a spectrum, the cuvette with the solution was thermostatted for 25-30 min at the given temperature. A second record of the spectrum at the same temperature completely coincided with the first one. The accuracy of temperature measurements was ±0.5°C. To avoid evaporation of the solvent at high temperatures, a vaseline oil layer was poured above the studied solution. Concentrated NaOH and HCl solutions were used for pH titration of RTX-SII solution. pH was measured using a pH meter from InoLab (WTW GmbH, Germany); the accuracy of measurements was ±0.02. In the peptide spectral region ellipticity was calculated in the units deg·cm^2·dmol^{-1} as ellipticity of the average protein residue, assuming the average molecular mass of the amino acid residue as 110 daltons and using the formula: $[\theta] = [\theta]_{obs} \cdot S \cdot 110/10 \cdot C \cdot l$, where S is sensitivity of the scale of the spectropolarimeter, C is protein concentration (mg/ml), and l is the optical path length (mm). In the aromatic spectral region ellipticity was calculated as the molar ellipticity $[\theta]_M$ with molecular mass of actinoporin RTX-SII 19.28 kD. The spectropolarimeter was calibrat-

ed with 0.06% ammonium d-camphor-10-sulfonate. The ratio of ellipticity of the bands at 191 and 290 nm was 2.05.

Fluorescence spectra of RTX-SII were recorded using a Hitachi 850 spectrofluorimeter (Hitachi, Japan) in 1-cm pathlength quartz cuvettes. The effect of the ionic strength on the fluorescence spectra was studied by addition of a certain amount of concentrated NaCl solution to a cuvette with actinoporin solution. The wavelengths of excitation were 280 and 296 nm. The fluorescence spectra corrected using rhodamine B from Wako Pure Chemical Industries (Japan) were recorded with subtraction of the Raman band of the buffer solution. The fluorescence intensity was corrected for volume increase on heating and addition of concentrated NaCl solution. The widths of the slits of the excitation and emission monochromators were set for 5 nm spectral resolution.

RESULTS AND DISCUSSION

The UV spectrum of RTX-SII in the near UV region (230-350 nm) is a typical protein spectrum with a maximum at 275 nm and a minimum near 250 nm. A clearly detected shoulder at about 290 nm indicates that there are a significant number of tryptophan residues in the amino acid content of actinoporin (spectrum not presented here).

The values of $A^{1\%}_{1\ cm}$ determined from UV spectra of RTX-SII solutions in 0.01 M sodium phosphate buffer, pH 7.2, and in 6 M guanidine hydrochloride, pH 4.0, at 275 nm with correction for light scattering (3-5% at the absorption maximum) are 15.5 and 16.3, respectively. The corresponding molar extinction coefficients are 29,890 and 31,430 $M^{-1}\cdot cm^{-1}$. The numbers of tyrosine and tryptophan residues evaluated using the second derivative of the UV spectra [21] are 11 and 3, respectively. The molar extinction coefficient calculated from these data agrees well with that measured from the UV spectrum of RTX-SII solution.

The CD spectrum of RTX-SII in the near UV region (230-310 nm), the absorption region of the aromatic chromophores and disulfide bonds (Fig. 1a), has positive bands at 284 and 290 nm related with the tyrosine and/or tryptophan residues. The presence of a distinct fine structure of the CD spectrum of RTX-SII in the near UV region indicates that there is a significant asymmetry in the environment of the side groups of the aromatic amino acid residues, that is, they are constrained, and, consequently, the studied polypeptide has a highly organized tertiary structure.

The CD spectrum of RTX-SII in the far UV region (190-240 nm)—the absorption region of peptide bonds (Fig. 1b)—has a minimum at 217 nm and a maximum at 198 nm, the curve crossing the base line twice, at 195 and 203 nm. Calculation of the secondary structure elements of RTX-SII using Provencher's program [22] gives the following content of canonical structures: 5% α-helix, 48% antiparallel folded β-sheets, 26% β-turns, and 22% unordered structure. Thus, a predominance of β-sheet is typical of the structural organization of actinoporins; this was also found for equinatoxins and sticholysins by CD and IR spectroscopy [23-25] and proved by X-ray structural analysis [26, 27].

Effect of temperature on RTX-SII conformation. On increasing the temperature from 25 to 40°C, the ellipticity of the bands of the CD spectrum of actinoporin RTX-SII in the absorption region of the aromatic amino acid residues decreases by 5-7% (Fig. 1a). Increasing temperature to 50°C results in a drastic decrease in ellipticity of the bands in the 250-270 nm region. It is obvious that a conformational transition in the tertiary structure of actinoporin occurs at 40-50°C. Further heating of the solution (up to 60°C) does not result in significant changes in the CD spectrum of RTX-SII. The actinoporin molecule seems to be in a partially denatured stable state. Cooling to 25°C of RTX-SII solution incubated at 60°C and its incubation for two days at 25°C results in a partial restoration of ellipticity of the bands of CD spectrum (25-30% of the initial value).

Along with "melting" of the tertiary structure of actinoporin RTX-SII, the CD spectra in the absorption region of the peptide bonds indicate that its secondary structure also destroyed on increasing temperature (Fig. 1b): a negligible decrease in ellipticity of the negative and positive bands of the spectrum is observed at 50°C. Increasing temperature by only 5°C results in drastic changes in the CD spectrum: 60% decrease in ellipticity of the positive and negative bands with a wavelength shift of the maximum, minimum, and a cross-point of the base line is observed (Fig. 1b). Heating of actinoporin solution to 60°C results in further decrease in ellipticity of the negative band and disappearance of the maximum in the positive spectral region.

A point of conformational transition in the secondary structure of RTX-SII is determined from an ellipticity plot at 222 nm versus temperature (Fig. 1c), the former being a measure of ordering of the secondary structure of protein [28]. As shown in Fig. 1c, the ellipticity of actinoporin does not depend on temperature in the range 20-45°C and then drastically decreases over a narrow temperature range. The midpoint of this transition corresponds to 53°C. Below this temperature conformational changes in the tertiary as well as secondary structures are completely reversible. It should be noted that above this point of conformational transition, changes in the tertiary structure are partially reversible, whereas changes in the secondary structure are completely irreversible.

The CD spectra of actinoporin RTX-SII recorded in the range 25-60°C (Fig. 1a) do not have an isodichroic point (intersection of all curves at the same point at a cer-

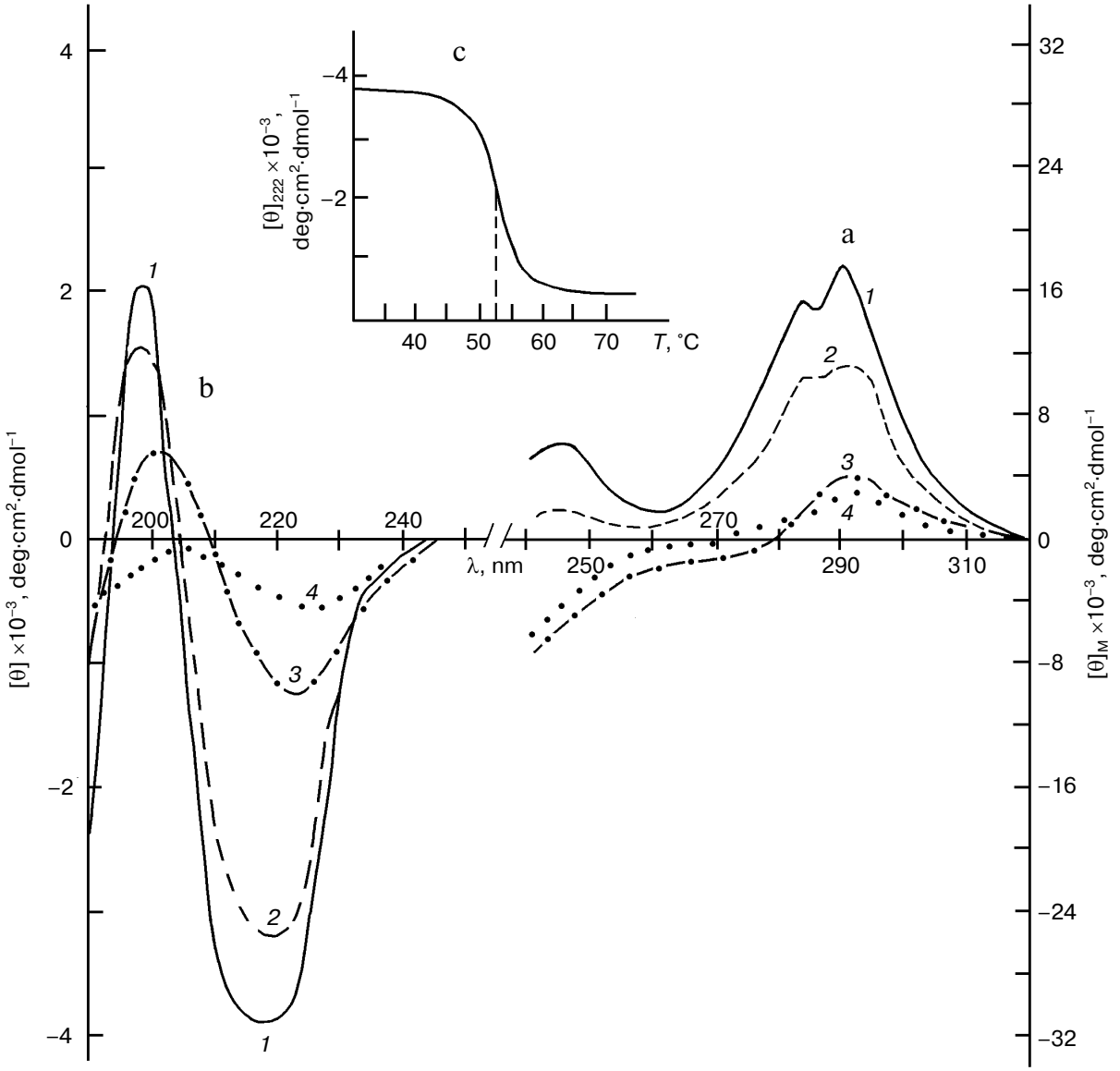

Fig. 1. CD spectra of actinoporin RTX-SII in 0.01 M sodium phosphate buffer, pH 7.2, at different temperatures (°C): *1*) 25; *2*) 50; *3*) 55; *4*) 60. Polypeptide concentration (mg/ml): 0.37 (a); 0.222 (b). c) Ellipticity of the band at 222 nm versus temperature.

tain wavelength [29]). This fact suggests that denaturation of actinoporin does not proceed in one stage (the presence of only native or denatured states), but an intermediate product is formed.

Effect of pH on the conformational state of RTX-SII. Along with the study of conformational thermal stability of RTX-SII, the effect of pH on the spatial structure of actinoporin was also investigated. The CD spectra of RTX-SII solutions (Fig. 2a) illustrate that the tertiary structure of the actinoporin is very stable both in acidic and basic pH regions. On pH decrease, the CD spectrum of RTX-SII in the near UV area retains its form and ellipticity of the bands. At pH 2.2, the ellipticity of the bands at 284 and 290 nm decreases by ~10%, but the spectrum retains its fine structure. On increasing pH the CD spectrum of actinoporin does not significantly change up to pH 11.7, excluding the range 240-260 nm. In this wavelength region a wide positive band typical of ionized tyrosine residues appears. Formation of a band with high ellipticity at 242 nm on increasing pH to 12.6 (Fig. 2a) indicates that the tyrosine residues in the RTX-SII molecule are completely ionized [30].

The secondary structure of actinoporin RTX-SII is as stable to pH changes as the tertiary structure. This is proved by the CD spectra in the peptide region (230-310 nm) recorded at various pH values (Fig. 2b). In acidic solutions (pH 5.0), a negligible decrease in ellipticity (by modulus) of the negative band at 217 nm is observed.

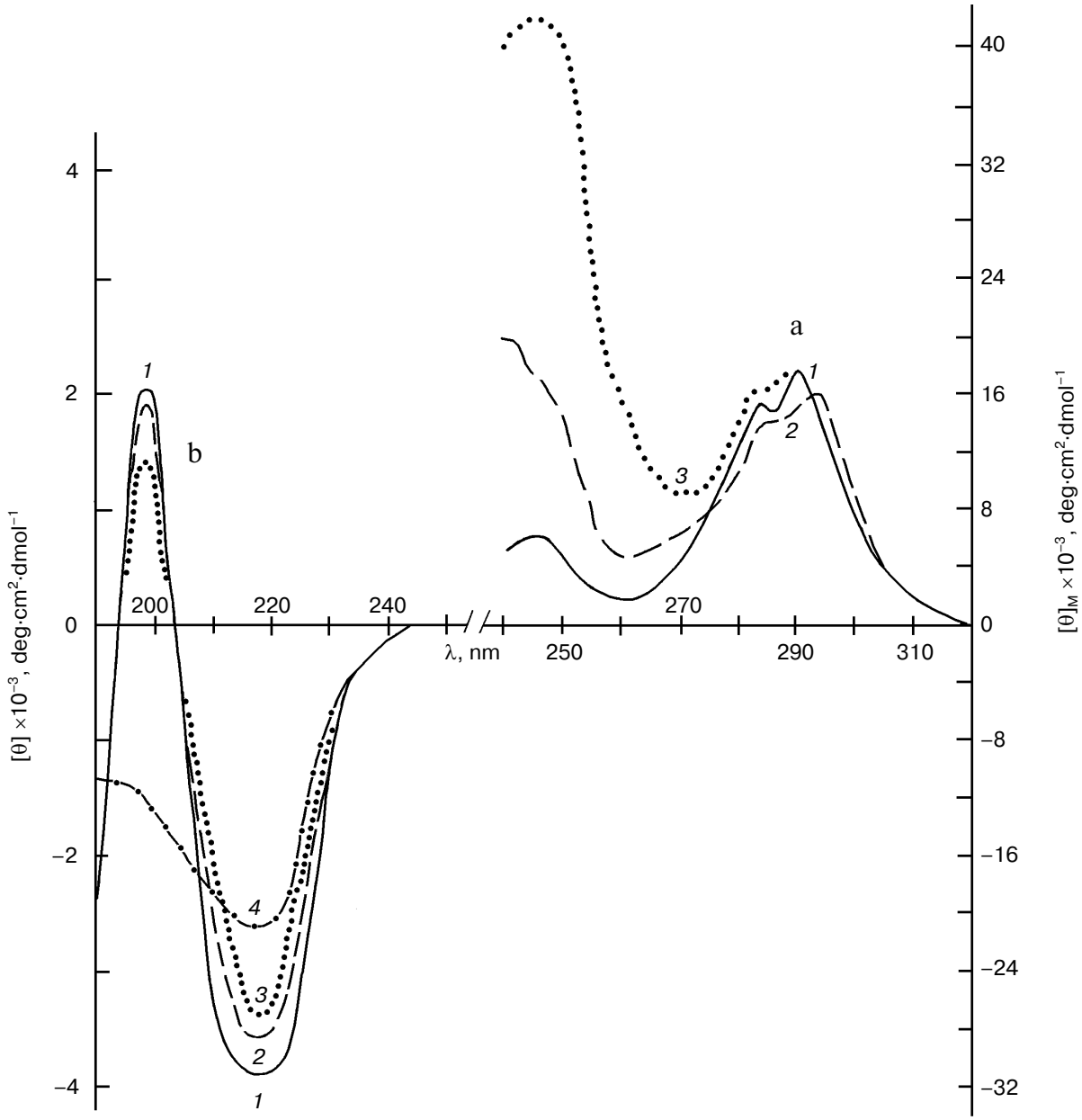

Fig. 2. CD spectra of actinoporin RTX-SII in 0.01 M sodium phosphate buffer at 25°C. a) Polypeptide concentration, 0.37 mg/ml. pH values: *1*) 7.2; *2*) 11.7; *3*) 12.6. b) Polypeptide concentration, 0.222 mg/ml. pH values: *1*) 7.2; *2*) 5.0; *3*) 1.7; *4*) 12.3.

Further pH decrease to 1.7 results in 10% decrease in ellipticity of the positive and negative bands in the CD spectrum of the polypeptide compared with the initial spectrum (pH 7.2).

Increasing pH from 7.2 to 10.4 does not cause changes in the peptide region of the CD spectra of RTX-SII. At pH 11.4, a drastic decrease in ellipticity of the negative band at 198 nm is observed, whereas ellipticity at 217 nm does not change. Further titration of the solution to pH 12.3 results in 30% decrease in ellipticity of the negative band at 217 nm and complete disappearance of the positive band (Fig. 2b).

To calculate the elements of the secondary structure of the samples of actinoporin RTX-SII subjected to effects of pH and temperature, we used the Contin program [22] and the CDPro package [31], which were developed for analysis of the secondary structure of globular proteins using CD spectra in the far UV region. In contrast to Contin (the Provencher and Glockner method), CDPro (the Sreerama and Woody method) used expanded sets of a various reference spectra; some of them contain CD spectra of denatured proteins. The CDPro package detects α-helix and β-sheet in two modifications: regular and distorted.

The contents of actinoporin secondary structure elements are shown in the table. As can be seen, the secondary structure of actinoporin RTX-SII in the native state (pH 7.2, 25°C) calculated using Contin differs from that calculated using CDPro in a higher content of β-sheet. Heating of RTX-SII solution to 55 and 60°C results in denaturation of the native polypeptide: the CD spectra recorded at these temperatures significantly differ from the initial one (Fig. 1b). According to the calculations by the Provencher and Glockner method, on increase in the degree of denaturation, the β-sheet content increases to 66% and the unordered form content decreases to 1% in the secondary structure of the polypeptide. This is unusual on denaturation of water-soluble membrane-active proteins to which actinoporins belong. Thus, for example, denaturation of equinatoxin EqtII and sticholisin StII is accompanied by increase in the α-helix content [24, 32] and decrease in the β-sheet content [32]. That is why we also used CDPro for calculations of the secondary structure of RTX-SII.

Calculation of the elements of secondary structure of RTX-SII using CDPro indicates that denaturation on heating results in a slight decrease in the α-helix content and more significant increase in the unordered form content (7-15%). The total β-sheet content is nearly unchanged, but redistribution of the regular and distorted fractions of β-sheet occurs: the content of distorted β-sheet increases (table).

Fluorescence of RTX-SII. The intrinsic fluorescence of actinoporin RTX-SII arises from three tryptophan and 11 tyrosine residues present in the molecule (calculated using the second derivative of the UV absorption spectrum as described in [21]). The fluorescence spectra of RTX-SII in 0.01 M sodium phosphate buffer, pH 7.2, at λ_{ex} = 280 and 296 nm are presented in Fig. 3. As known, at λ_{ex} = 280 nm there occurs emission of both tyrosine and tryptophan residues, that is, the total fluorescence, whereas excitation at 296 nm results in emission of only tryptophan residues [33]. The total fluorescence spectrum of RTX-SII is characterized by a maximum at 333 nm (Fig. 3, solid curve); the maximum of the tryptophan fluorescence spectrum is shifted to the red region by 6 nm (Fig. 3, dashed curve). The ratio of quantum yields of the total and tryptophan fluorescence is 3.5. This fact indicates that in the studied polypeptide, in which disulfide bonds are lacking, tyrosine residues significantly contribute to emission at λ_{ex} = 280 nm. This is an significant difference between actinoporin RTX-SII and equinatoxin II, sticholisin II [34, 35], and most of native globular proteins in which fluorescence of the tryptophan residues dominates at λ_{ex} = 280 nm due to quenching of emission of the tyrosine residues by various quencher [33].

As shown by the CD spectra in the near UV region (Fig. 1a), the tertiary structure of actinoporin RTX-SII is significantly temperature-dependent. Thus, it was of

Elements of the secondary structure of actinoporin RTX-SII, %

T, °C	pH	α-helix*			β-sheet*			β-turns	Unordered form
		I	II	III	I	II	III		
Provencher and Glockner method [22]									
25	7.2	—	—	5.0	—	—	48.0	26.0	22.0
50	7.2	—	—	1.0	—	—	52.0	23.0	25.0
55	7.2	—	—	0.0	—	—	60.0	29.0	10.0
60	7.2	—	—	0.0	—	—	66.0	33.0	1.0
25	2.0	—	—	0.0	—	—	53.0	27.0	21.0
25	12.3	—	—	2.0	—	—	56.0	28.0	14.0
Sreerama and Woody method [31]									
25	7.2	0.5	3.5	4.0	24.4	12.5	36.9	22.2	36.8
50	7.2	0.2	2.9	3.1	20.4	16.5	36.9	18.3	41.8
55	7.2	0.1	2.7	2.8	12.3	23.2	35.5	18.0	43.7
60	7.2	0.1	2.3	2.4	10.0	28.5	38.5	8.0	51.1
25	5.0	0.2	4.0	4.2	26.8	14.0	40.8	21.8	33.2
25	2.0	0.1	3.6	3.7	24.4	12.5	36.9	19.4	40.0
25	12.3	0.1	2.8	2.9	11.5	21.4	32.9	17.8	46.2

* I-III designate regular, distorted, and total structure, respectively.

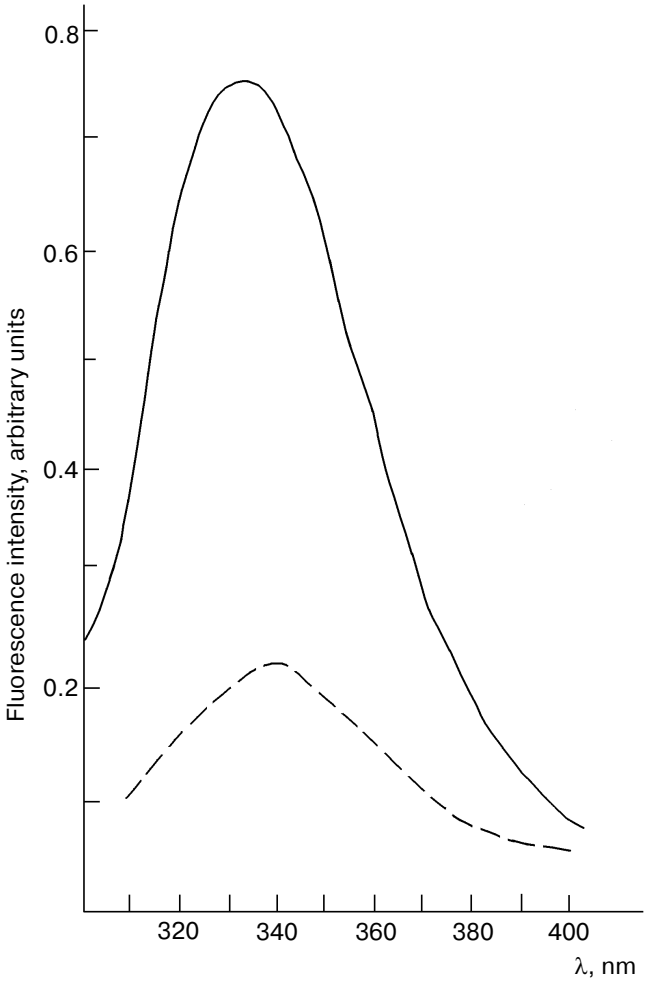

Fig. 3. Fluorescence spectra of actinoporin RTX-SII (concentration $5 \cdot 10^{-8}$ M) in 0.01 M sodium phosphate buffer, pH 7.2. Solid and dashed curves correspond to total (λ_{ex} = 280 nm) and tryptophan (λ_{ex} = 296 nm) fluorescence.

interest to analyze the temperature dependence of the intrinsic fluorescence spectra of RTX-SII. Heating of actinoporin solutions from 25 to 70°C results in decrease in intensity both total and tryptophan fluorescence (Fig. 4a); the intensity of total fluorescence changes more sharply than that of tryptophan fluorescence. Intensity decrease in the RTX-SII fluorescence spectra at increased temperature is accompanied by a red shift of the maximum by 8-11 nm (Fig. 4a). This fact indicates that the tyrosine and tryptophan residues become more solvent-accessible, which is caused by unfolding of the actinoporin molecule on heating [33].

As shown earlier, the hemolytic activity of actinoporin depends on the ionic strength of the solution [32]. Increase in the ionic strength of actinoporin solution by titration with 5 M NaCl influences both the total and tryptophan fluorescence of RTX-SII (Fig. 4b). The intensity of the total fluorescence spectrum of RTX-SII increases at NaCl concentration 0.025 M, and a second drastic intensity increase is observed at 0.4 M NaCl. Further increase in the ionic strength of RTX-SII solution does not result in a fluorescence intensity change (Fig. 4b, curve *1*). Ionic strength-dependent increase in the total fluorescence intensity occurs with a stable spectral maximum (333 nm) (data not presented here).

The intensity of tryptophan fluorescence changes negligibly on increase in the ionic strength. In solutions with up to 0.1 M NaCl concentration the emission smoothly increases and does not change on further increase in the ionic strength (Fig. 4b, curve *2*). However, with sufficiently small changes in intensity of tryptophan fluorescence, the spectral maximum shifts to 335 nm (blue shift). This fact indicates that at high NaCl concentrations the indole group of tryptophan is surrounded by nonpolar amino acid residues of the molecule [36].

Hemolytic activity. Determination of hemolytic activity using various animal erythrocytes is widely used in functional studies of actinoporins [3, 8, 15, 24] and other pore-forming toxins [19].

The effect of temperature on RTX-SII activity is illustrated in Fig. 5. With increasing temperature, the activity of actinoporin decreases, and RTX-SII is com-

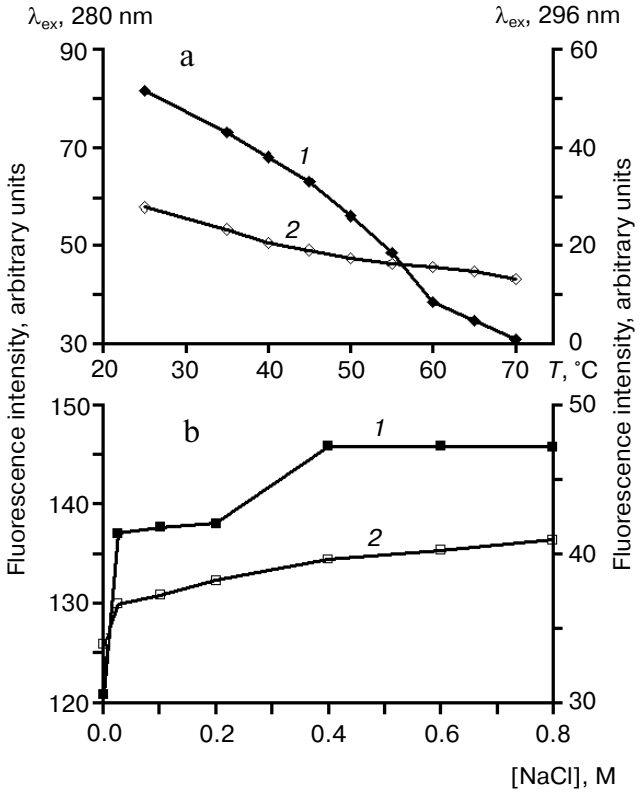

Fig. 4. Dependence of fluorescence of actinoporin RTX-SII in 0.01 M sodium phosphate buffer, pH 7.2, on temperature (a) and ionic strength (b): *1*) total fluorescence (left ordinate); *2*) tryptophan fluorescence (right ordinate).

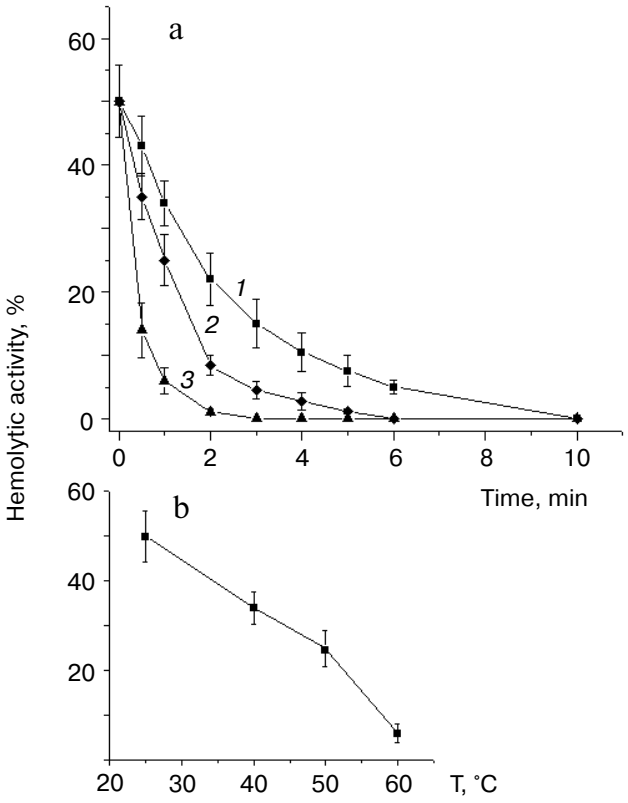

Fig. 5. Dependence of hemolytic activity of actinoporin RTX-SII on incubation time (a) and temperature (b). Temperature (°C): *1*) 40; *2*) 50; *3*) 60. Incubation time, 1 min (b). Here and in Fig. 6 the standard deviations (±S.D.) are based on the results of three independent experiments.

pletely inactivated on incubation for 3 min at 60°C (Fig. 5a). The hemolytic activity of the polypeptide drastically decreases above the temperature of conformational transfer of actinoporin (53°C) (Fig. 5b). The hemolytic activity of RTX-SII obviously depends on the conformational state of the molecule and is related with its secondary and tertiary structures.

The pH dependence of hemolytic activity of RTX-SII is shown in Fig. 6a. Hemolytic activity of the polypeptide does not change in the pH range from 4 to 6.5. Drastic increase in activity is observed at pH from 6.7 to 7.6 and further small increase at pH from 8.0 to 10.2. Changes in the tertiary structure occurring at high pH and change in the molecule charge (pI ~ 10) seem to promote the process of pore formation. An analogous effect of high pH on activity of actinoporins was demonstrated for cytosin CIII from *S. helianthus* [37] and colenterolysin from *Phymactis clematis* [38].

Dependence of hemolytic activity of RTX-SII on the ionic strength of the solution is presented in Fig. 6b. Increase in NaCl concentration to 0.8 M results in a noticeable increase in hemolytic activity of actinoporin. This is probably caused by some changes in the tertiary structure of the polypeptide; these changes are indicated by the total and tryptophan fluorescence spectra (Fig. 4b). Increase in the intrinsic fluorescence intensity is obviously related with change in the charge of polypeptide molecule as well as that of the amino acid residues directly surrounding tyrosine and tryptophan residues. An analogous effect is observed for equinatoxin II and sticholisin I and is explained by facility of partial unfolding of the polypeptide in solution with high NaCl concentration [32, 39].

Thus, our studies demonstrate that RTX-SII, like other actinoporins, has a significantly constrained tertiary structure and an ordered secondary structure with high β-sheet content. The secondary structure of the polypeptide is retained essentially unchanged over a wide pH range (from 2.0 to 11.7), whereas certain changes in the tertiary structure occur at the alkaline titration; this is caused by ionization of the tyrosine residues. The observed increase in pore-forming capacity of actinoporin seems to be caused by changes in the molecular conformation. Irreversible denaturation of the polypeptide resulting in complete loss of its activity is observed at temperature above 53°C. Increase in the ionic strength of the solution results in changes in its tertiary structure and increase in

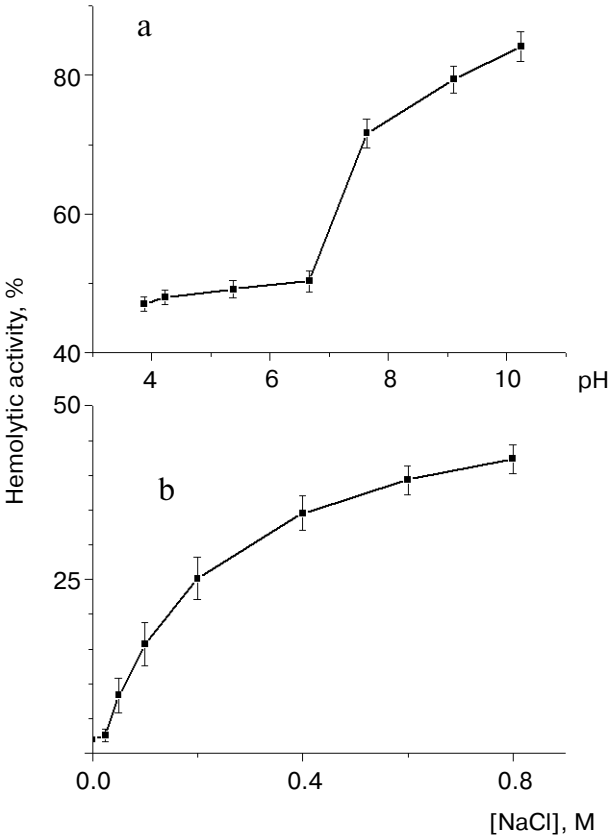

Fig. 6. Dependence of the hemolytic activity of actinoporin RTX-SII on pH (a) and ionic strength of the solution (b).

the hemolytic activity of the actinoporin. The tyrosine residues in the RTX-SII molecule significantly contribute to emission of the polypeptide, and their fluorescence is more dependent on temperature and the ionic strength of solution than tryptophan fluorescence.

This work was financially supported by the Russian Foundation for Basic Research (grant No. 02-04-49486) and the Presidium of Russian Academy of Sciences, program "Molecular and Cellular Biology" (grant No. 03-1-0-05-002).

REFERENCES

1. Norton, R. S. (1998) *J. Toxicol.-Toxin Rev.*, **17**, 99-130.
2. Macek, P. (1992) *Microbiol. Immunol.*, **105**, 121-130.
3. Turk, T. (1991) *J. Toxicol.-Toxin Rev.*, **10**, 223-262.
4. Galettis, P., and Norton, R. S. (1990) *Toxicon*, **28**, 695-706.
5. Batista, U., Macek, P., and Sedmak, B. (1986) *Period. Biol.*, **88**, 97-98.
6. Tejica, M., Anderluh, G., Macek, P., Marcet, R., Torres, D., Sarracent, J., Alvarez, C., Lanio, M. E., Serra, M. D., and Menestrina, G. (1999) *Int. J. Parasitol.*, **29**, 489-498.
7. Chanturiya, A. N. (1990) *Biochim. Biophys. Acta*, **1026**, 248-250.
8. Shnyrov, V. L., Monastyrnaya, M. M., Zhadan, G. G., Kuznetsova, S. M., and Kozlovskaya, E. P. (1992) *Biochem. Int.*, **26**, 219-229.
9. Zhadan, G. G., Kuznetsova, S. M., Opalikova, O. V., Monastyrnaya, M. M., Zykova, T. A., Emelyanenko, V. I., Villar, E., and Shnyrov, V. L. (1994) *Biochem. Mol. Biol. Int.*, **32**, 331-340.
10. Anderluh, G., and Macek, P. (2002) *Toxicon*, **40**, 111-124.
11. Anderluh, G., Krizaj, I., Strukelj, B., Gubensek, F., Macek, P., and Pungercar, J. (1999) *Toxicon*, **37**, 1391-1401.
12. Norton, R. S., Bobek, G., Ivanov, J. O., Thomson, M., Fiala-Beer, E., Moritz, R. L., and Simpson, R. J. (1990) *Toxicon*, **28**, 29-41.
13. Huerta, V., Morera, V., Guanche, Y., Cinea, G., Gonzales, L. J., Betancourt, L., Martinez, D., Alvarez, C., Lanio, M. E., and Besada, V. (2001) *Toxicon*, **39**, 1253-1256.
14. Khoo, K. S., Kam, W. K., Khoo, H. E., Gopalakrishnakone, P., and Chung, M. C. M. (1993) *Toxicon*, **31**, 1567-1579.
15. Monastyrnaya, M. M., Zykova, T. A., Apalikova, O. W., Shwets, T. W., and Kozlovskaya, E. P. (2002) *Toxicon*, **40**, 1197-1217.
16. Klyshko, E. V., Il'yna, A. P., Likhatskaya, G. N., Issaeva, M. P., Guzev, K. V., Monastyrnaya, M. M., Kozlovskaya, E. P., Lipkin, A. V., Barsova, E. I., Kryzko, E. V., Trifonov, E. V., and Nurminsky, E. A. (2004) *Vestnik DVO RAN*, **3**, 45-53.
17. Klyshko, E. V., Issaeva, M. P., Monastyrnaya, M. M., Il'yna, A. P., Guzev, K. V., Vakorina, T. I., Dmitrenok, P. S., Zykova, T. A., and Kozlovskaya, E. P. (2004) *Toxicon*, **44**, 315-326.
18. Lowry, O. H., Rosebrough, N. J., Farr, A. L., and Randall, R. J. (1951) *J. Biol. Chem.*, **193**, 265-275.
19. Kitagava, I., Nishino, T., Kobayashi, M., and Kyogoku, Y. (1981) *Chem. Pharm. Bull.*, **29**, 1951-1956.
20. Winder, A. F., and Gent, W. L. G. (1971) *Biopolymers*, **10**, 1243-1251.
21. Ichikawa, T., and Johnson, C. Yr. (1983) *Chem. Pharm. Bull.*, **29**, 438-444.
22. Provencher, S. W., and Glockner, W. C. (1981) *Biochemistry*, **20**, 33-37.
23. Belmonte, G., Menestrina, G., Pederzolli, C., Krizaj, I., Gubensek, F., Turk, T., and Macek, P. (1994) *Biochim. Biophys. Acta*, **1192**, 197-204.
24. Poklar, N., Lah, J., Salobir, M., Macek, P., and Vesnaver, G. (1997) *Biochemistry*, **36**, 14345-14352.
25. Menestrina, G., Cabiaux, V., and Tejuca, M. (1999) *Biochem. Biophys. Res. Commun.*, **254**, 174-180.
26. Athanasiadis, A., Anderluh, G., Macek, P., and Turk, D. (2001) *Structure*, **9**, 341-346.
27. Mancheno, J. M., Martin-Benito, J., Martinez-Ripoll, M., Gavilanes, J. G., and Hermoso, J. A. (2003) *Structure*, **11**, 1-20.
28. Ven'yaminov, S. Yu., Kosykh, V. G., Kholodkov, O. A., and Bur'yanov, Ya. I. (1990) *Bioorg. Khim.*, **16**, 47-51.
29. France, L. L., Kieleczawa, J. J., Dunn, J. J., Hind, G., and Sutherland, J. C. (1992) *Biochim. Biophys. Acta*, **1120**, 59-68.
30. Moroz, S. V., Glazunov, V. P., Vakorina, T. I., Pavlenko, A. F., Odinokov, S. E., and Ovodov, Yu. S. (1987) *Bioorg. Khim.*, **13**, 519-527.
31. http:/lamar.colostate.edu/~sreeram/CDPro
32. Alvarez, C., Lanio M. E., Tejuca, M., Martinez, D., Pazos, F., Campos, A. M., Encinas, M. V., Pertinhez, T., Schreier, S., and Lissi, E. A. (1998) *Toxicon*, **36**, 165-178.
33. Lakovich, D. (1986) *Basics of Fluorescence Spectroscopy* [Russian translation], Mir, Moscow.
34. Macek, P., Zecchini, M., Pederzolli, C., Serra, M. D., and Menestrina, G. (1995) *Eur. J. Biochem.*, **234**, 329-335.
35. Alvarez, C., Pazos, I. F., Lanio, M. E., Martinez, D., Schreier, S., Casallanovo, F., Campos, A. M., and Lissi, E. (2001) *Toxicon*, **39**, 539-553.
36. Eftink, M. R. (1998) *Biochemistry* (Moscow), **63**, 276-284.
37. Doyle, J. W., and Kem, W. R. (1989) *Biochim. Biophys. Acta*, **987**, 181-186.
38. Meinardi, E., Azcurra, J. M., Florin-Christensen, M., and Florin-Christensen, J. (1994) *Comp. Biochem. Physiol.*, **109B**, 153-161.
39. Macek, P., and Lebez, D. (1981) *Toxicon*, **19**, 233-240.